Semiconductor Physics, Quantum Electronics & Optoelectronics, 2021. V. 24, No 4. P. 419-424.

Hetero- and low-dimensional structures

Analytic theory for current-voltage characteristic of a nanowire radial *p-i-n* diode

V.L. Borblik

V. Lashkaryov Institute of Semiconductor Physics, NAS of Ukraine,
41, prospect Nauky, 03680 Kyiv, Ukraine; e-mail: borblik@isp.kiev.ua

Abstract. In this article, process of current flow in a nanowire radial *p-i-n* diode has been considered in detail. It has been shown that cylindrical geometry of the structure gives rise to specific asymmetry of the concentration distribution for current carriers injected to the *i*-layer, which is opposite to asymmetry that is due to inequality of carriers' mobilities. This specific asymmetry rises with bringing the *i*-layer nearer to the nanowire center. Together with that, decrease of the current density in a "long" *p-i-n* diode and its increase in a "short" *p-i-n* diode take place (at given forward voltage). And variation of radial thickness of the *i*-layer demonstrates maximums in the current density at the thickness close to the bipolar diffusion length.

Keywords: core-shell nanowire, radial *p-i-n* diode, concentration distribution, current-voltage characteristic.

https://doi.org/10.15407/spqeo24.04.419
PACS 62.33.Hj, 73.03.-b, 85.30.Kk

Manuscript received 04.06.21; revised version received 15.07.21; accepted for publication 10.11.21; published online 23.11.21.

1. Introduction

In the recent time, there is permanently growing interest of the researchers in multilayer semiconductor nanowires with a radial structure of the layers obtained by their different doping or/and making the heterostructures. These structures have large perspectives for usage in variety of new (core-shell) nanoelectronic devices: solar cells [1–5], photodetectors [6], nanowires for energy harvesting [7], field-effect transistors [8], high electron mobility devices [9], nanowire-based light-emitting diodes [10], nanowire lasers [11] *etc*.

The most of these nanowire devices contain radial *p-n* or *p-i-n* junctions and use the transverse transport through them. Due to cylindrical symmetry of these structures, their electronic properties acquire a number of peculiarities in comparison with analogous planar devices. In particular, distribution of the non-equilibrium carriers injected into base layer of the radial *p-n* junction diode decays with a different rate depending on the injection direction – from the nanowire center to periphery or *vice versa* [12]. The reason is overlaying of specific concentration falling with radial coordinate related to cylindrical geometry of the structure onto its falling due to recombination. This circumstance results in, respectively, increasing or decreasing the diode saturation current as compared with analogous planar diode. And electric field in the *i*-layer of radial *p-i-n* diode proves to be inhomogeneous primordially, decaying from the nanowire center that was shown in Ref. [13] by simulation and in Ref. [14] analytically. All these peculiarities enlarge with decreasing the nanowire radius.

Though in the most of cases, the large arrays of the same type nanowires are used in applications, it is useful to investigate in detail the properties of single radial *p-n* or *p-i-n* elements for the sake of their optimization [15]. The fact is that radial *p-i-n* diodes contain (in the frame of single device) both injection directions: from the nanowire center and to it. Therefore, it is of interest to consider their transport properties in whole.

In this article, the spatial distribution of current carriers injected to middle layer of a radial *p-i-n* diode and its forward current-voltage characteristic are calculated analytically because simulation by means of standard programs does not give full solution of the problem.

2. Spatial distribution of current carriers injected to the *i*-layer

A schematic view of the structure under consideration is shown in Fig. 1, where *i*-layer is located between r_1 and r_2; r_p and r_n are the depletion region boundaries. Basic equations of the task are continuity equations

$$divI_n = R\,, \tag{1}$$

$$divI_p = -R\,. \tag{2}$$

© 2021, V. Lashkaryov Institute of Semiconductor Physics, National Academy of Sciences of Ukraine

Here, $R = \frac{n}{\tau} = \frac{p}{\tau}$ describes recombination (τ is a lifetime of the non-equilibrium carriers, the high injection level is supposed, *i.e.* $n(r) = p(r)$), and partial electron and hole currents are

$$I_n = q\left(D_n \mathrm{grad}(n) + \mu_n n(r) E(r)\right), \tag{3}$$

$$I_p = q\left(-D_p \mathrm{grad}(p) + \mu_p p(r) E(r)\right), \tag{4}$$

where q is the electron charge, D_n, D_p, μ_n, μ_p are electron and hole diffusion coefficients and mobilities, $E(r)$ is radial electric field.

In our calculation, we will follow to approach used in paper [16] for consideration of a planar *p-i-n* diode. It is assumed that at the borders of the highly doped *p*- and *n*-regions, the current I is carried only by holes or electrons, respectively:

$$I_p(r_1) = I, \tag{5}$$

$$I_n(r_1) = 0, \tag{6}$$

$$I_p(r_2) = 0, \tag{7}$$

$$I_n(r_2) = I. \tag{8}$$

According to (7),

$$I_p(r_2) = q\mu_p\left(-\theta \left.\frac{dp}{dr}\right|_{r=r_2} + p(r_2)E(r_2)\right) = 0,$$

where $\theta = kT/q$ (k is the Boltzmann constant, T – temperature), whence

$$E(r_2) = \frac{\theta}{p(r_2)} \left.\frac{dp}{dr}\right|_{r=r_2}. \tag{9}$$

Then according to (6),

$$I_n(r_1) = q\mu_n\left(\theta \left.\frac{dn}{dr}\right|_{r=r_1} + n(r_1)E(r_1)\right) = 0,$$

whence it follows that

$$E(r_1) = -\frac{\theta}{n(r_1)} \left.\frac{dn}{dr}\right|_{r=r_1}. \tag{10}$$

Next, according to (5) with using (10)

$$I_p(r_1) = q\mu_p\left(-\theta \left.\frac{dp}{dr}\right|_{r=r_1} + p(r_1)E(r_1)\right) = -2q\mu_p\theta \left.\frac{dn}{dr}\right|_{r=r_1} = I,$$

whence

$$\left.\frac{dn}{dr}\right|_{r=r_1} = -\frac{I}{2q\mu_p\theta}, \tag{11}$$

and according to (8) with using (9)

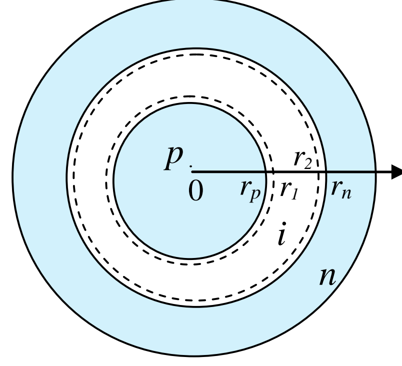

Fig. 1. Schematic view of a radial *p-i-n* diode.

$$I_n(r_2) = q\mu_n\left(\theta \left.\frac{dn}{dr}\right|_{r=r_2} + n(r_2)E(r_2)\right) = 2q\mu_n\theta \left.\frac{dn}{dr}\right|_{r=r_2} = I,$$

whence it follows that

$$\left.\frac{dn}{dr}\right|_{r=r_2} = \frac{I}{2q\mu_n\theta}. \tag{12}$$

Equations (1) and (2) are reduced in natural way to ambipolar discontinuity equation

$$\mathrm{div}\left[\mathrm{grad}(n)\right] = \frac{n(r)}{D_{amb}\tau}$$

which under conditions of cylindrical symmetry takes the form

$$\frac{1}{r}\frac{d}{dr}\left(r\frac{dn}{dr}\right) = \frac{n(r)}{D_{amb}\tau}, \tag{13}$$

where $D_{amb} = \left(\mu_p D_n + \mu_n D_p\right)/\left(\mu_n + \mu_p\right)$. Solution of Eq. (13) is

$$n(r) = C_1 I_0\left(r/L_{amb}\right) + C_2 K_0\left(r/L_{amb}\right), \tag{14}$$

where $L_{amb} = \sqrt{D_{amb}\tau}$, I_0 and K_0 are modified Bessel functions of 1st and 2nd kind, respectively. Introducing new variable $x = r/L_{amb}$, we obtain for derivative of (14)

$$\frac{dn}{dx} = C_1 I_1(x) - C_2 K_1(x). \tag{15}$$

Integration constants C_1 and C_2 have to be determined from (11) and (12) as the boundary conditions:

$$\left.\frac{dn}{dx}\right|_{x=x_1} = C_1 I_1(x_1) - C_2 K_1(x_1) = -\frac{IL_{amb}}{2q\mu_p\theta}, \tag{16}$$

$$\left.\frac{dn}{dx}\right|_{x=x_2} - C_1 I_1(x_2) - C_2 K_1(x_2) = \frac{IL_{amb}}{2q\mu_n\theta}. \tag{17}$$

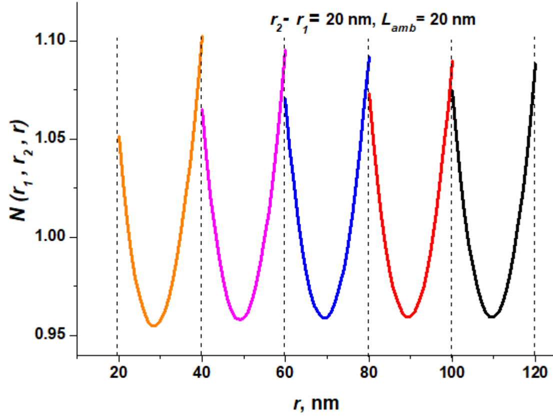

Fig. 2. Spatial distribution of non-equilibrium carriers in the *i*-layer at different its positions relatively to the nanowire center.

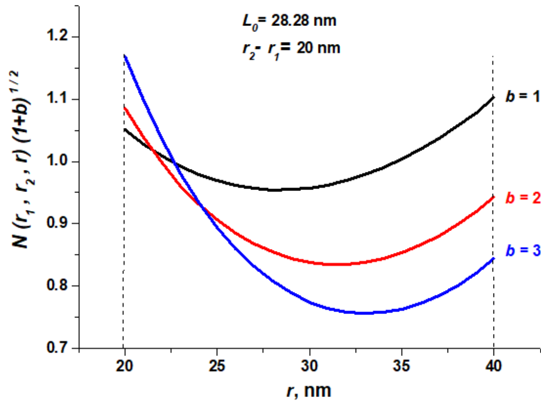

Fig. 3. Spatial distribution of non-equilibrium carriers in the *i*-layer at different values of the mobility ratio.

Finally, we obtain

$$n(x) = \frac{I\tau}{qL_{amb}(1+b)\Delta} \times \\ \times \{[K_1(x_1) + bK_1(x_2)]I_0(x) + [I_1(x_1) + bI_1(x_2)]K_0(x)\}, \tag{18}$$

where $\Delta = I_1(x_2)K_1(x_1) - I_1(x_1)K_1(x_2)$, $b = \mu_n/\mu_p$.

Spatial distribution (18) of carriers injected to *i*-layer is characterized by dimensionless factor

$$N(r_1, r_2, r) = \frac{1}{(1+b)\Delta} \times \\ \times \{[K_1(x_1) + bK_1(x_2)]I_0(x) + [I_1(x_1) + bI_1(x_2)]K_0(x)\}.$$

As an example, Fig. 2 represents this factor at radial thickness of the *i*-layer equal to 20 nm, the same value of diffusion length L_{amb} and $b = 1$ in different positions of the *i*-layer relative to nanowire center. In contrast to the case of planar *p-i-n* diode [17], in radial *p-i-n* diode, the concentration distribution of non-equilibrium carriers proves to be asymmetrical even at $\mu_n = \mu_p$ and this asymmetry grows with going of the *i*-layer nearer to the nanowire center.

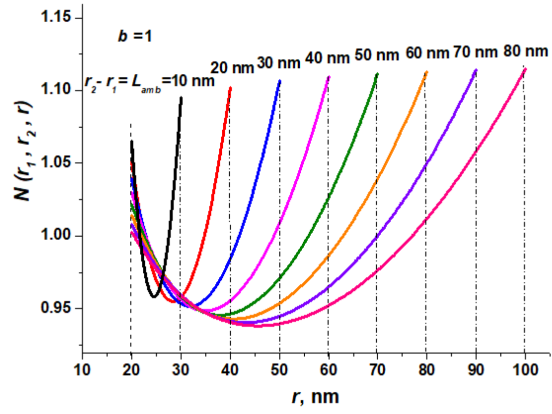

Fig. 4. Dependence of spatial distribution of non-equilibrium carriers in the *i*-layer on its radial thickness, when it coincides with bipolar diffusion length (at $b = 1$).

In order to study dependence of the carrier distribution on mobility ratio b, it is also necessary to take into account the dependence of the ambipolar diffusion length itself on b:

$$L_{amb} = \sqrt{D_{amb}\tau} = \sqrt{\frac{2D_n\tau}{1+b}} \equiv \frac{L_0}{\sqrt{1+b}}. \tag{19}$$

Fig. 3 illustrates the spatial distribution of non-equilibrium carriers in the *i*-layer with the radial thickness 20 nm at different values of parameter b when $L_0 = 20\sqrt{2}$ nm (that gives $L_{amb} =$ 20 nm at $b = 1$ as in Fig. 2). It is seen from this figure that $b > 1$ inverts the asymmetry character suppressing the asymmetry, which is due to cylindrical geometry of the structure.

It is also of interest to track how distribution asymmetry due to cylindrical geometry enlarges with increasing radial thickness of the *i*-layer when L_0 is kept equal to the thickness. These dependences are presented in Fig. 4.

3. The forward current-voltage characteristic

Under conditions of Boltzmann statistics, we have at the left edge of *i*-layer

$$\frac{p(r_1)}{n_i} = \frac{n(r_1)}{n_i} = e^{\frac{qU_l}{kT}} \tag{20}$$

and at the right one –

$$\frac{n(r_2)}{n_i} = \frac{p(r_2)}{n_i} = e^{\frac{qU_r}{kT}}, \tag{21}$$

where

$$n(r_1) = \frac{I\tau}{qL_{amb}(1+b)\Delta} \times \\ \times \{[K_1(x_1) + bK_1(x_2)]I_0(r_1) + [I_1(x_1) + bI_1(x_2)]K_0(r_1)\} \equiv \\ \equiv \frac{I\tau}{qL_{amb}(1+b)\Delta}\{\ \}_1,$$

$$n(r_2) = \frac{I\tau}{qL_{amb}(1+b)\Delta}\times$$
$$\times\{[K_1(x_1)+bK_1(x_2)]I_0(r_2)+[I_1(x_1)+bI_1(x_2)]K_0(r_2)\}\equiv$$
$$\equiv\frac{I\tau}{qL_{amb}(1+b)\Delta}\{\ \}_2 .$$

Multiplying (20) and (21), one can obtain an expression for the current in the form

$$I = \frac{qL_{amb}n_i}{\tau}\frac{(1+b)\Delta}{\sqrt{\{\ \}_1\{\ \}_2}}e^{\frac{q(U_l+U_r)}{2kT}} . \tag{22}$$

Under introducing the total voltage $U = U_l + U_m + U_r$, where U_m is a voltage drop across the i-layer, the current-voltage characteristic takes the form

$$I = \frac{qL_{amb}\,n_i}{\tau}\frac{(1+b)\Delta}{\sqrt{\{\ \}_1\{\ \}_2}}e^{-\frac{qU_m}{2kT}}e^{\frac{qU}{2kT}}\equiv$$
$$\equiv\frac{qL_{amb}\,n_i}{\tau}F(r_1,r_2)e^{\frac{qU}{2kT}} , \tag{23}$$

where dependence of the current-voltage characteristics on position and thickness of the i-layer is described by the factor $F(r_1,r_2)$.

A voltage drop across the i-layer is given as $U_m = \int_{r_1}^{r_2} E(r)dr$, where radial electric field $E(r)$ is determined from Eqs. (3) and (4) after their summation

$$E(r) = \frac{I}{q(1+b)\mu_p n(r)} - \frac{(b-1)\theta}{(b+1)n(r)}\frac{dn}{dr} . \tag{24}$$

The dependence of current density on the position of i-layer relatively to the nanowire center (determined by the factor $F(r_1,r_2)/\sqrt{(1+b)}$, when accounting also its dependence on the mobility ratio) is different at different relationships between the radial thickness of i-layer and bipolar diffusion length. Figs 5a, 5b, 5c illustrate this dependence. It is seen from these figures that bringing the i-layer nearer to the nanowire center reduces the current density at $L_0 < r_2 - r_1$ (a case of "long" diode), almost does not change it at $L_0 \approx r_2 - r_1$ and enlarges it at $L_0 > r_2 - r_1$ (a case of "short" diode).

The role of relationship between the radial thickness $r_2 - r_1$ of i-layer and diffusion length L_{amb} manifests itself even brighter in dependence of the current density on radial extent of the i-layer at given L_{amb} (Fig. 6). The value of current density is maximal, when $r_2 - r_1$ is of the order of bipolar diffusion length (but larger than it) and decays in both sides from this region. And the maximum values decrease with the mobility ratio.

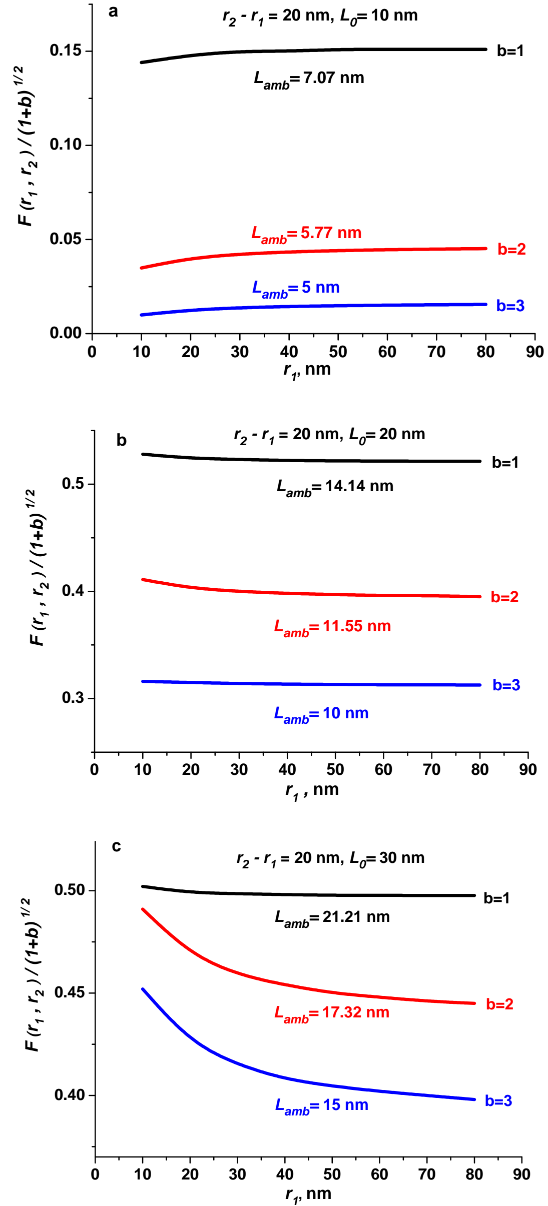

Fig. 5. Dependences of the current density on i-layer position relatively to the nanowire center at $L_0 < r_2 - r_1$ (a), $L_0 \approx r_2 - r_1$ (b), and $L_0 > r_2 - r_1$ (c).

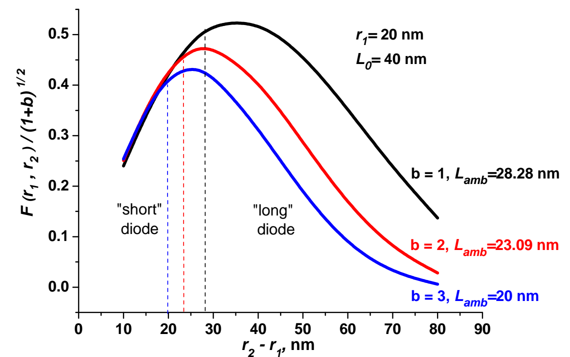

Fig. 6. Dependences of the current density on radial extent of the i-layer at given value of bipolar diffusion length.

4. Conclusion

Cylindrical geometry of radial *p-i-n* diode results in its own (“geometrical”) asymmetry of the concentration distribution in the diode middle region opposite to asymmetry that is caused by mobility inequality. This asymmetry increases with bringing the *i*-layer nearer to the nanowire center. At the same time, decreasing the current density in the “long” *p-i-n* diode and its increasing in the “short” *p-i-n* diode take place. And at the radial thickness of *i*-layer, which approaches to the bipolar diffusion length, the current density manifests a maximum value. Above behavior may be important for photovoltaic applications.

References

1. Tian B., Zheng X., Kempa T.J., Fang Y., Yu N., Yu G., Huang J., and Lieber C.M. Coaxial silicon nanowires as solar cells and nanoelectronic power sources. *Nature.* 2007. **449**. P. 885–890. https://doi.org/10.1038/nature06181.
2. Colombo C., Heiβ M., Grätzel M., and Fontcuberta i Morral A. Gallium arsenide *p-i-n* radial structures for photovoltaic applications. *Appl. Phys. Lett.* 2009. **94**, No 17. P. 173108. https://doi.org/10.1063/1.3125435.
3. Dong Y., Tian B., Kempa T.J., and Lieber C.M. Coaxial group III-nitride nanowire photovoltaics. *Nano Lett.* 2009. **9**, No 5. P. 2183–2187. https://doi.org/10.1021/nl900858v.
4. Yoo J., Dayeh S.A., Tang W., and Picraux S.T. Epitaxial growth of radial Si *p-i-n* junctions for photovoltaic applications. *Appl. Phys. Lett.* 2013. **102**, No 9. P. 093113. https://doi.org/10.1063/1.4794541.
5. Zhang Y., Sanchez A.M., Aagesen M. *et al*. Growth and fabrication of high-quality single nanowire devices with radial *p-i-n* junctions. *Small.* 2019. **15**, No 3. P. 1803684. https://doi.org/10.1002/smll.201803684.
6. Soci C., Zhang A., Bao X.-Y., Kim H., Lo Y., and Wang D. Nanowire photodetectors. *J. Nanosci. Nanotechnol.* 2010. **10**, No 3. P. 1430–1449. https://doi.org/10.1166/jnn.2010.2157.
7. Goktas N.I., Wilson P., Ghukasyan A., Wagner D., McNamee S., and LaPierre R.R. Nanowires for energy: A review. *Appl. Phys. Rev.* 2018. **5**, No 4. P. 041305. https://doi.org/10.1063/1.5054842.
8. Xiang J., Lu W., Hu Y., Wu Y., Yan H., and Lieber C.M. Ge/Si nanowire heterostructures as high-performance field-effect transistors. *Nature*. 2006. **441**. P. 489–493. https://doi.org/10.1038/nature04796.
9. Jiang X., Xiong Q., Nam S., Qian F., Li Y., and Lieber C.M. InAs/InP radial nanowire heterostructures as high electron mobility devices. *Nano Lett.* 2007. **7**, No 10. P. 3214–3218. https://doi.org/10.1021/nl072024a.
10. Tomioka K., Motohisa J., Hara S., Hiruma K., and Fukui T. GaAs/AlGaAs core multishell nanowire-based light-emitting diodes on Si. *Nano Lett.* 2010. **10**, No 5. P. 1639–1644. https://doi.org/10.1021/nl9041774.
11. Hua B., Motohisa J., Kobayashi Y., Hara S., and Fukui T. Single GaAs/GaAsP coaxial core-shell nanowire lasers. *Nano Lett.* 2009. **9**, No 1. P. 112–116. https://doi.org/10.1021/nl802636b.
12. Borblik V.L. Effect of circular *p-n* junction curvature on the diode current density. *J. Electron. Mater.* 2016. **45**, No 8. P. 4117–4121. https://doi.org/10.1007/s11664-016-4597-z.
13. Christesen J.D., Zhang X., Pinion C.W., Celano T.A., Flynn C.J., and Cahoon J.F. Design principles for photovoltaic devices based on Si nanowires with axial or radial *p-n* junctions. *Nano Lett.* 2012. **12**, No 11. P. 6024–6029. https://doi.org/10.1021/nl303610m.
14. Borblik V.L. Electrostatics of nanowire radial *p-i-n* diode. *Semiconductor Physics, Quantum Electronics & Optoelectronics.* 2019. **22**, No 2. P. 201–205. https://doi.org/10.15407/spqeo22.02.201.
15. Tian B., Kempa T.J. and Lieber C.M. Single nanowire photovoltaics. *Chem. Soc. Rev.* 2009. **38**. P. 16–24. https://doi.org/10.1039/B718703N.
16. Benda H. and Spenke E. Reverse recovery processes in silicon power rectifiers. *Proc. IEEE*. 1967. **55**, No 12. P. 1331–1354. https://doi.org/10.1109/PROC.1967.6093.
17. Herlet A. The forward characteristic of silicon power rectifiers at high current densities. *Solid State Electron.* 1968. **11**, No 8. P. 717–742. https://doi.org/10.1016/0038-1101(68)90053-1.

Author and CV

Dr. Vitalii L. Borblik graduated from Kiev State University in 1968. He received his PhD in physics and mathematics from the Institute of Semiconductors, Academy of Sciences of UkrSSR in 1978. At present, he is senior scientific researcher of the Department of Electric and Galvanomagnetic Properties of Semiconductors at the V. Lashkaryov Institute of Semiconductor Physics. His researches include electron transport in semiconductor heterostructures, dynamical concentration lattices in bipolar semiconductor plasma, injection and exclusion phenomena in semiconductor devices and physics of the diode temperature sensors. Recent scientific interests of V.L. Borblik are electric and optic properties of nanostructured materials. He is the author of over 80 publications.
https://orcid.org/0000-0002-8224-9170

Аналітична теорія вольт-амперної характеристики нанодротового радіального *p-i-n* діода

В.Л. Борблик

Анотація. У роботі детально розглянуто процес струмоперенесення у нанодротовому радіальному *p-i-n* діоді. Показано, що циліндрична геометрія структури приводить до специфічної асиметрії розподілу концентрації інжектованих в *i*-шар носіїв струму, яка обернена до тої, що зумовлена нерівністю рухливостей носіїв. Ця специфічна асиметрія зростає з наближенням *i*-шару до центра нанодроту. При цьому відбувається зменшення густини струму в «довгому» *p-i-n* діоді та її збільшення в «короткому» (при даній прямій напрузі). А зміна радіальної товщини *i*-шару демонструє максимуми в густині струму при товщині, близькій до довжини біполярної дифузії.

Ключові слова: нанодріт типу ядро-оболонка, радіальний *p-i-n* діод, вольт-амперна характеристика.